

*Electronic Supplementary Information (ESI)*

**Dual-defective Strategy Directing In-situ Assembly for  
Effective Interfacial Contacts in MoS<sub>2</sub> Cocatalyst/In<sub>2</sub>S<sub>3</sub> Light  
Harvester Layered Photocatalyst**

**Zhibin Fang,<sup>a</sup> Xueyan Huang,<sup>a</sup> Yaozhu Wang,<sup>a</sup> Wenhui Feng,<sup>a</sup> Yan Zhang,<sup>a</sup>  
Sunxian Weng,<sup>b</sup> Xianzhi Fu<sup>a</sup> and Ping Liu<sup>\*a</sup>**

<sup>a</sup>State Key Laboratory of Photocatalysis on Energy and Environment, Research Institute of Photocatalysis, College of Chemistry, Fuzhou University, Fuzhou 350002, P. R. China.

<sup>b</sup>State Grid Fujian Electric Power Research Institute, Fuzhou 350002, P. R. China.

\*Corresponding author: Ping Liu

E-mail: liuping@fzu.edu.cn

Phone & Fax: +86-591-83779239

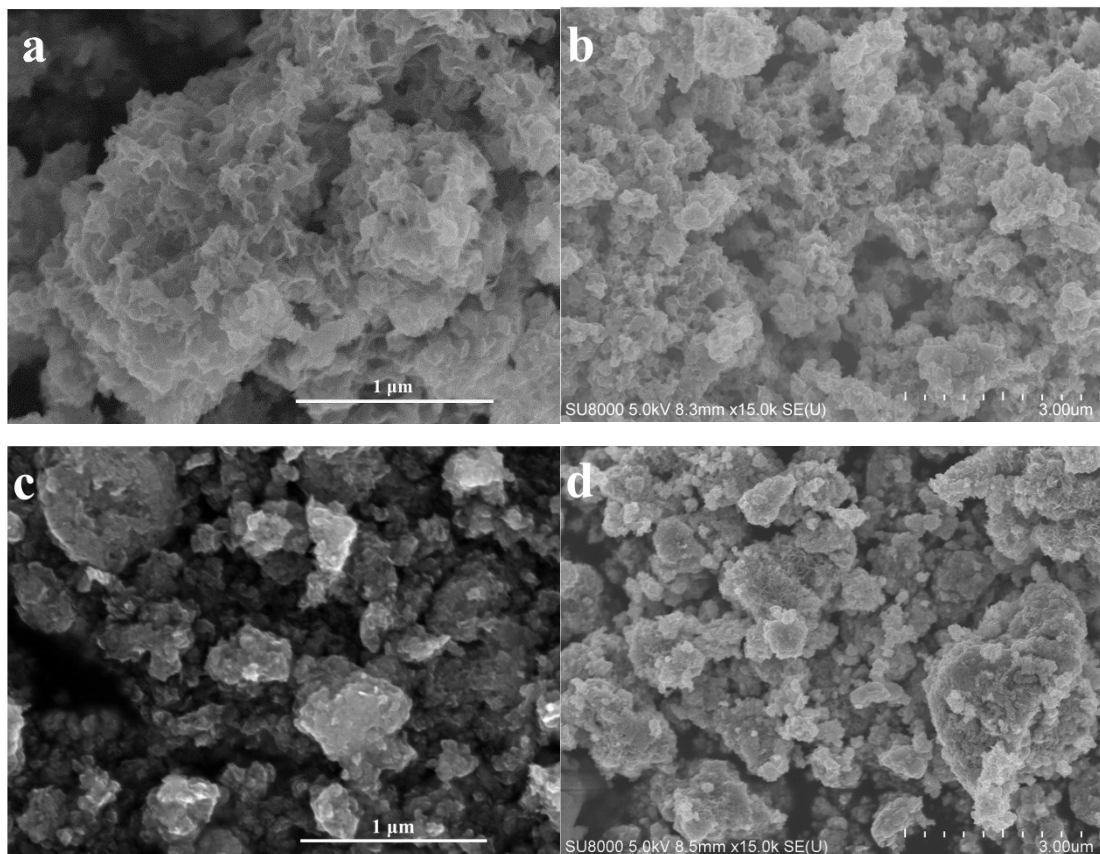


**Figure S1.** SEM images of the as-prepared samples with or without CTAB assistance: (a) and (b) IS (with CTAB); (c) and (d) b-IS (without CTAB).

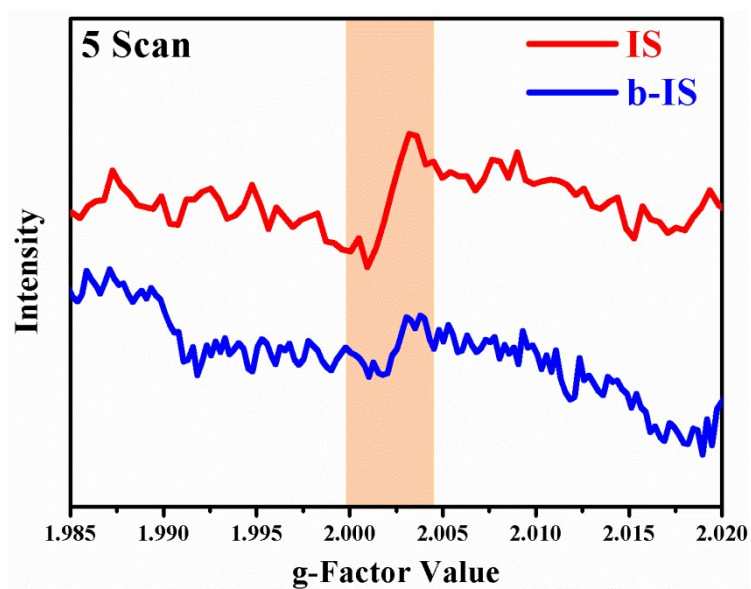


**Figure S2.** Intensified room-temperature ESR spectra conducted with 5 scans.

Since b-IS is not perfectly crystallized, trace amounts of defects like S vacancies should still exist in it. By increasing scan times, we can observe a faint ESR signal of S vacancies in b-IS sample, which is much weaker than that in IS sample (Figure S2). This result correlates with their different crystallinities revealed by XRD results.

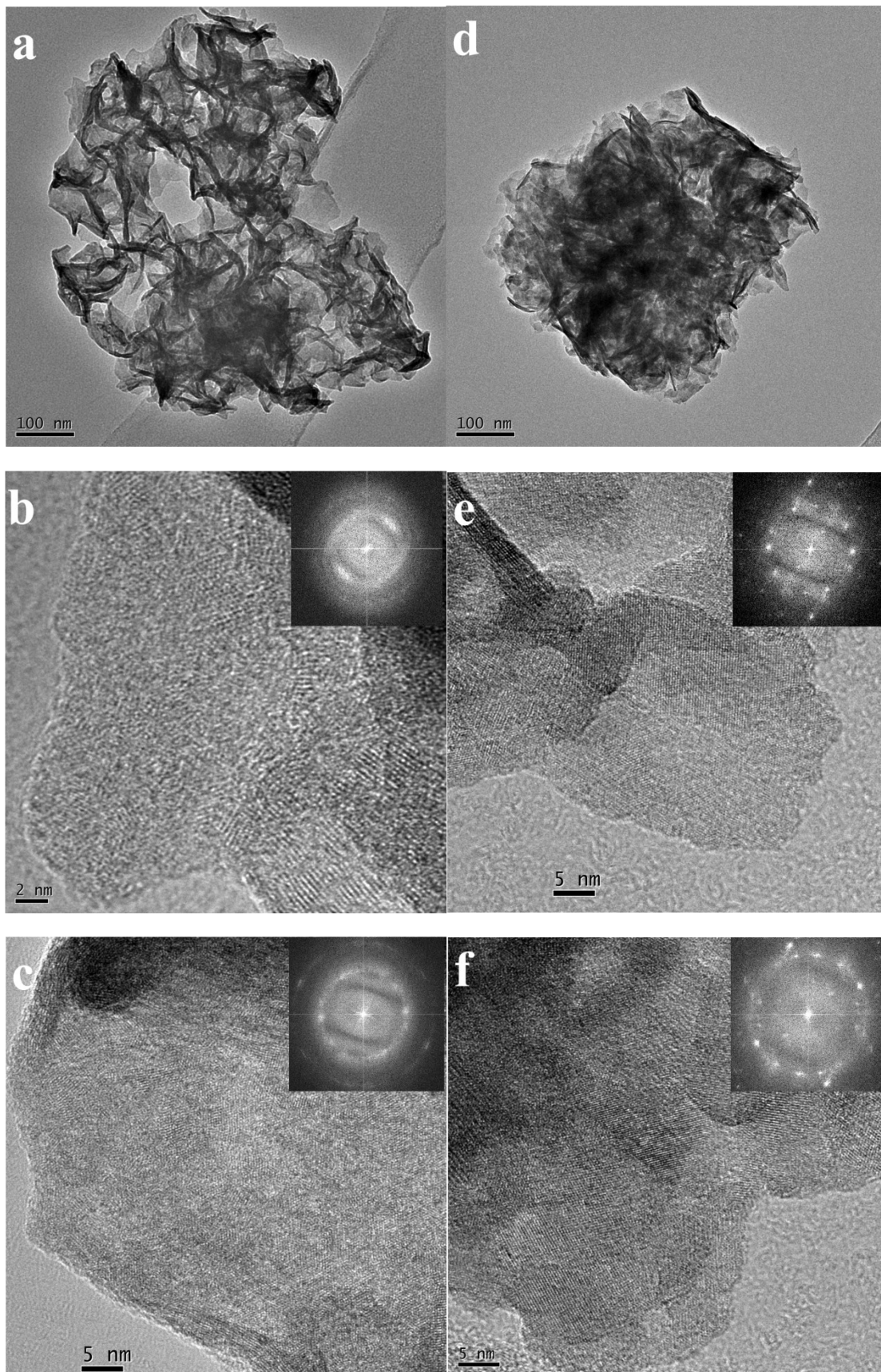


**Figure S3.** TEM and HRTEM images of In<sub>2</sub>S<sub>3</sub> samples with different disordered degrees: (a-c) IS sample; (d-f) b-IS samples; inserts: corresponding FFT patterns.



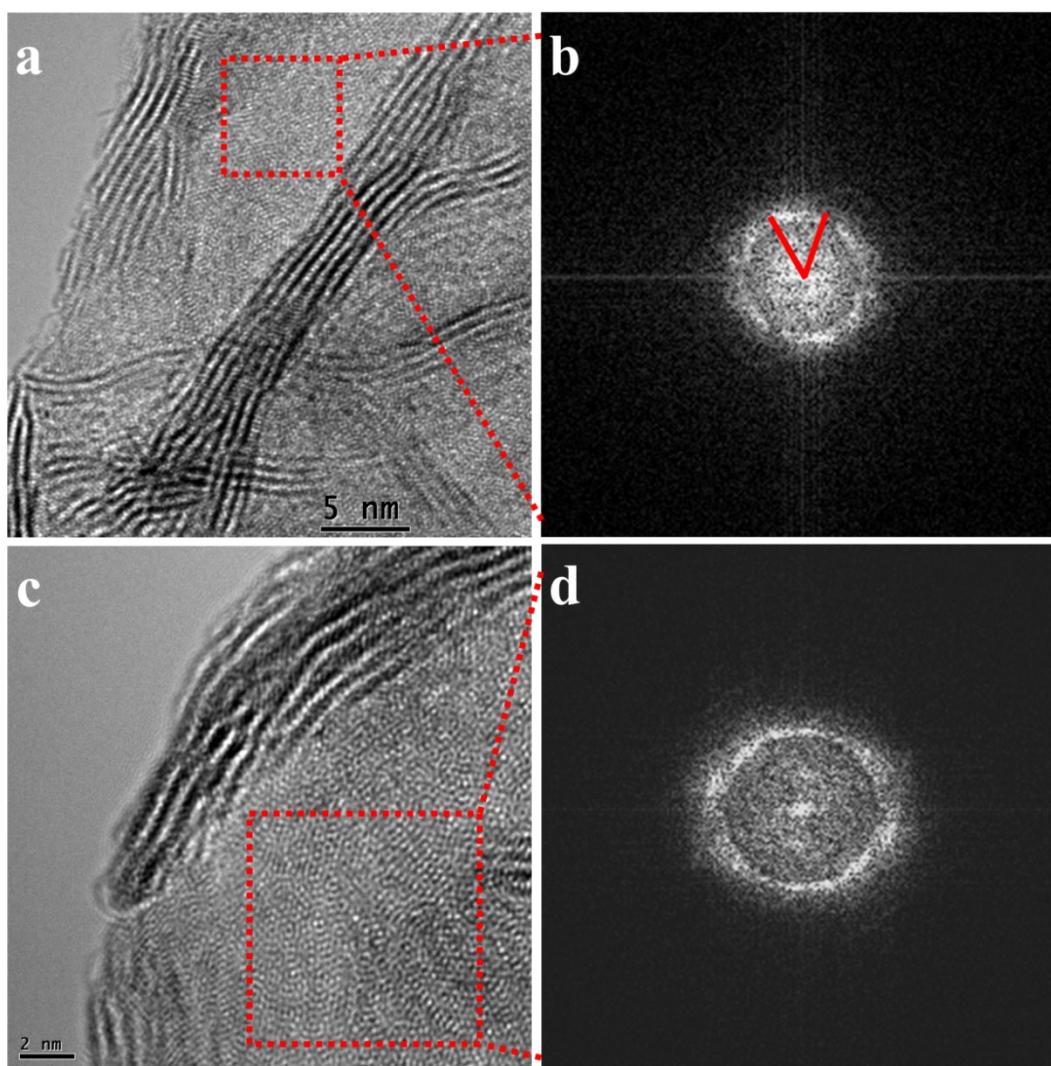


**Figure S4.** HRTEM images (a and b) and corresponding FFT patterns (c and d) for the as-prepared defective MoS<sub>2</sub> (dMS).

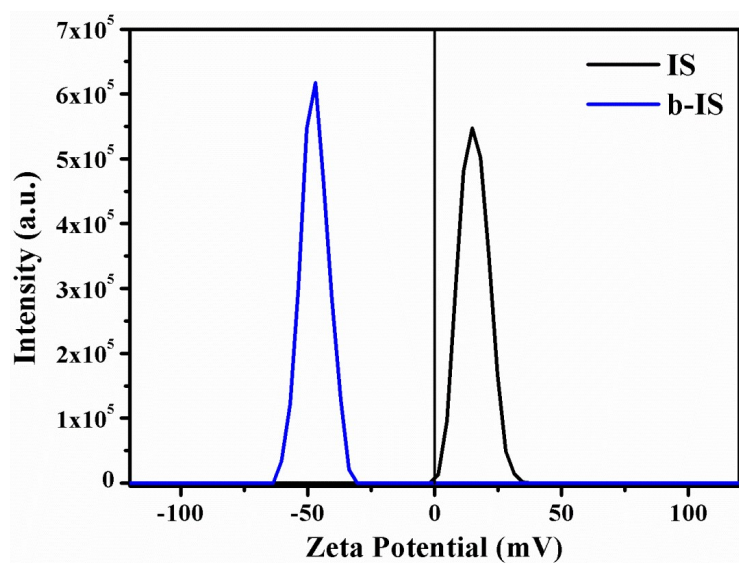


**Figure S5.** Zeta potentials of the as-prepared In<sub>2</sub>S<sub>3</sub> samples with or without CTAB assistance.

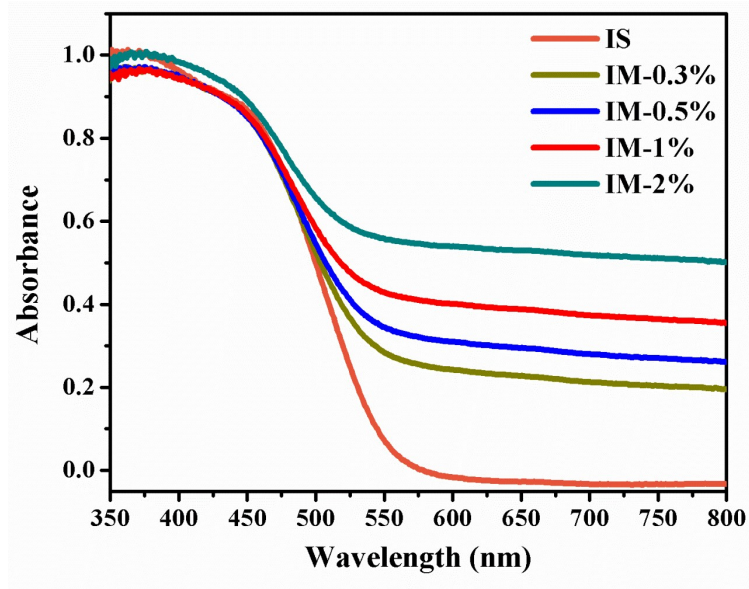


**Figure S6.** UV-vis diffuse reflectance spectra (DRS) of bare  $\text{In}_2\text{S}_3$  sample and composite samples loaded with varied amount of  $\text{MoS}_2$ .

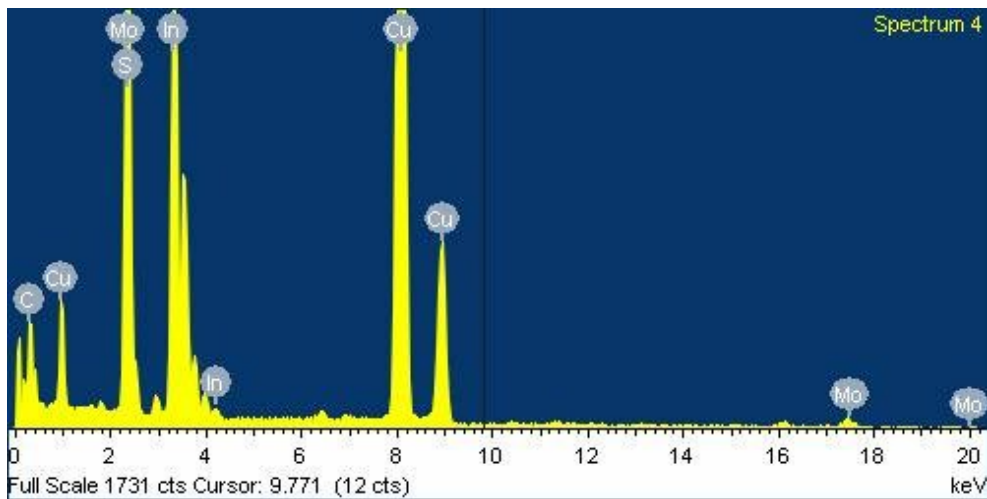


**Figure S7.** Energy dispersive spectroscopy (EDS) of IM-2% sample corresponding to Figure 5b.

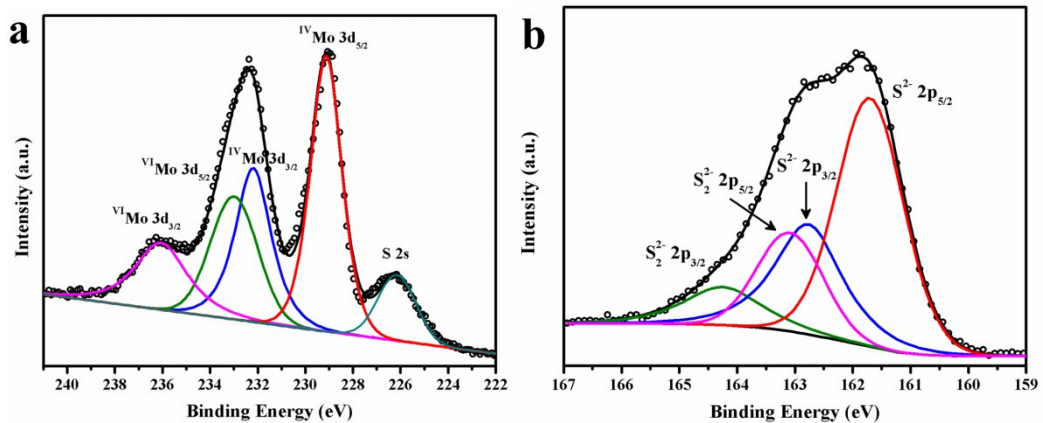


**Figure S8.** XPS spectra of Mo 3d orbitals (a) and S 2p orbitals (b) for defective  $\text{MoS}_2$  (dMS).

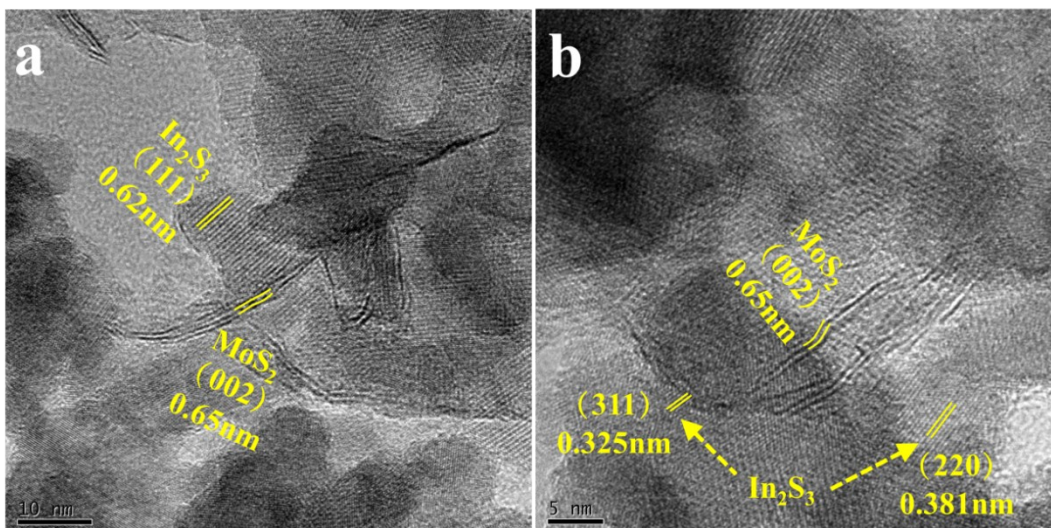


**Figure S9.** HRTEM images of b-IM1% sample.

**Table S1.** BET surface area of the samples

Sample	BET Surface Area (m <sup>2</sup> ·g <sup>-1</sup> )
IS	64.2005
IM-0.3%	66.9216
IM-0.5%	69.4746
IM-1%	67.2880
IM-2%	68.5181
b-IS	129.2601
b-IM1%	110.2031

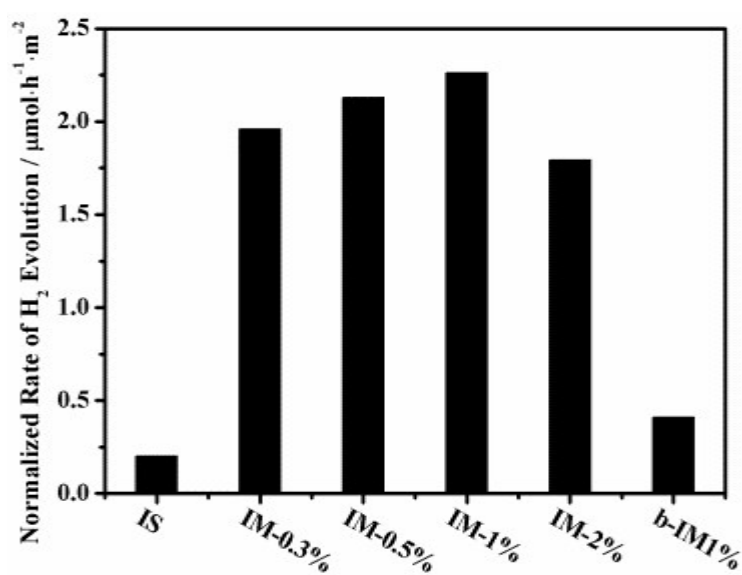


**Figure S10.** Surface-area-normalized rate of H<sub>2</sub> generation for the photocatalysts



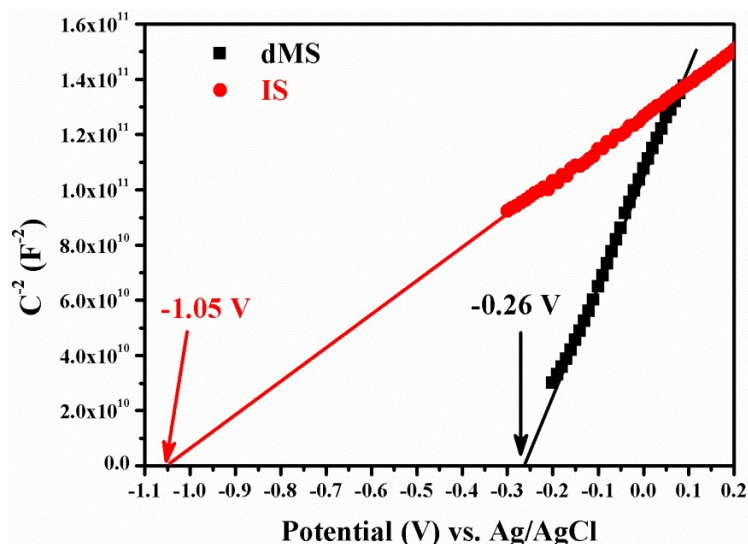


**Figure S11.** Mott-Schottky curves of IS electrode and dMS electrode.

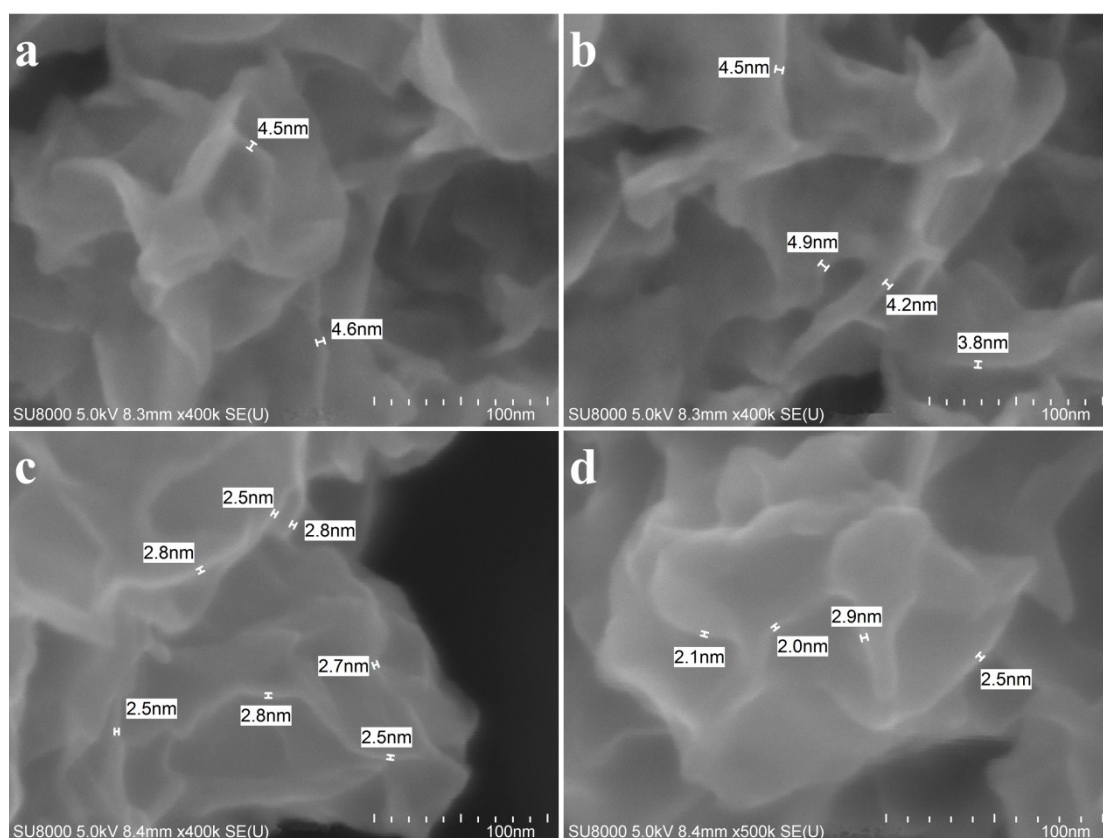


**Figure S12.** High-magnification SEM images of as-prepared IS (a and b) and dMS (c and d) sample for thickness measurements.

Measured from the following SEM images of IS sample (Figure S12ab in the revised ESI), the average thickness of  $\text{In}_2\text{S}_3$  nanosheets is 4.42 nm. Since the as-prepared  $\text{In}_2\text{S}_3$  nanosheets are not totally monodispersed but partially integrated with each other as shown in Figure 1a and Figure S1ab, it should be hard to define and measure the size of them. Likewise, the average thickness of  $\text{MoS}_2$  nanosheets is measured to be 2.55

nm, indicating a layer number of 4 for the as-prepared MoS<sub>2</sub> nanosheets. This is in accord with the HRTEM results in Figure 4d and Figure S4ac, confirming the few-layered nature of the defective MoS<sub>2</sub>.

**Table S2.** Data for the calculation of apparent quantum yields (AQYs) of IM-1% photocatalyst

Wavelength (nm)	Irradiance ( $\mu\text{W}\cdot\text{cm}^{-2}$ )	H <sub>2</sub> yield ( $\mu\text{L}/\text{h}$ )	AQY (%)
400	20599.97	59.9369	0.191
450	27962.15	62.1667	0.130
500	29000.49	22.8184	0.0413
550	31670.75	2.51	0.00379
600	34096.80	0	0
650	33753.42	0	0

The apparent quantum yield (AQY) was measured under the same photocatalytic reaction condition with incident light at different wavelengths by using band-pass filters ( $\lambda \pm 15$  nm) and a 300 W Xe lamp. The AQY was calculated according to the following equation:

$$AQY [\%] = \frac{2 \times \text{number of } H_2 \text{ molecules}}{\text{number of incident photons}} \times 100$$

$$= \frac{2 \times V_{H_2} / 22.4 \times N_A}{\frac{I \times A \times t}{hc/\lambda}} \times 100$$

in which  $V_{H_2}$  is volume of the produced H<sub>2</sub>,  $N_A$  is Avogadro's constant,  $I$  is the measured irradiance of incident light,  $A$  is the irradiation area (11.3 cm<sup>2</sup>),  $t$  is the irradiation time,  $h$  is Planck constant,  $c$  is the speed of light and  $\lambda$  is the wavelength of incident light.

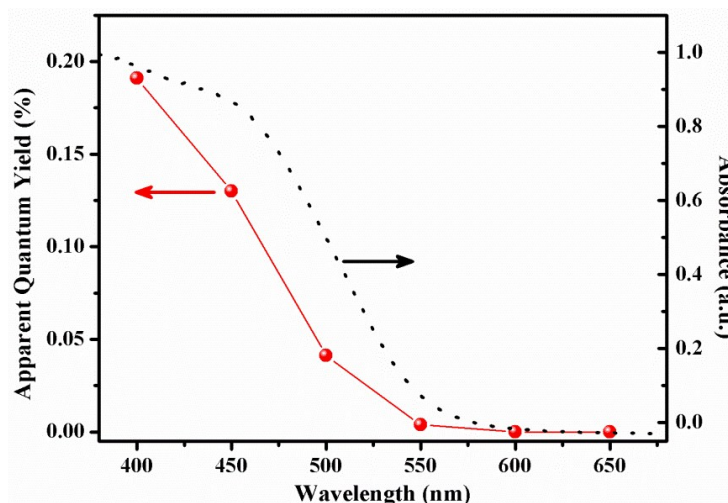




**Figure S13.** The light-absorbance-depended AQY distribution of IM-1% photocatalyst.

Although the AQYs of IM-1% at different monochromatic incident lights are low, a considerable dependence on the light absorbance is manifested obviously.

**Table S3.** Product Yields of as-prepared samples

Sample	IS	b-IS	IM-1%	b-IM1%	dMS	dMS-IM1%	cMS-IM1%
Yield	106.3%	94.0%	80.6%	89.8%	102.4%	114.2%	111.0%

Notably, yields of sample IS, dMS are greater than 100%, suggesting that the stoichiometric ratios of their composing elements should not exactly follow 2 : 3 for In : S and 1 : 2 for Mo : S due to their amorphous natures. And similar reasons can explain the cases of dMS-IM1% and cMS-IM1%, both of which undergo the fabrication process of amorphous  $\text{In}_2\text{S}_3$  (see in Experimental Details of the revised main text).